Size-dependent electronic structures of ZnO nanowires

Juan Wang, Xipo An, and Quan Li[a)]
Department of Physics, The Chinese University of Hong Kong, Shatin, New Territory, Hong Kong

R. F. Egerton
Department of Physics, University of Alberta, Edmonton, Canada TG 2J1

(Received 24 January 2005; accepted 29 March 2005; published online 12 May 2005)

ZnO nanowires with a diameter distribution from 20 to 100 nm were fabricated by a simple thermal evaporation process. Two different types of nanowire (circular versus hexagonal cross section) were obtained by controlling the growth conditions. The size-dependent electronic structures of both types of samples were investigated using valence electron energy-loss spectroscopy. Both the common features (surface plasmon, bulk plasmon width) and the differences (O 2*s* interband transition, bulk plasmon energy) between the two types of samples are discussed. The experimental results strongly suggest that ZnO nanowires with hexagonal cross section and low-index terminating surfaces are of high electronic quality, even at 20 nm diameter, and can thus serve as effective building blocks for optoelectronic nanodevices. © *2005 American Institute of Physics*.
[DOI: 10.1063/1.1927711]

Being one of the most important functional semiconductor materials, ZnO is found to have wide applications in the opto-electronic industry because of the material's excellent optical, electrical, and piezoelectrical properties.[1–3] Recently, its pseudo-one-dimensional (1D) nanostructures have attracted much attention due to their great potential to serve as functional building blocks for various nano-optoelectronic devices using the bottom-up approach.[4,5] It is known that material properties and thus the final performance of a device are mainly determined by its electronic states. Therefore, a fundamental understanding of the electronic structure of the 1D nanomaterial (in comparison to its bulk counterpart) is of primary concern.

Photoemission-based methods have been extensively used in the study of the electronic structure of the ZnO. Several interesting results have been reported, including dependence of the band-gap emission on the material size;[6,7] defect emission at ~500 nm enhanced by the presence of large surface areas,[8] and surface states observed at small ZnO size.[9–11] Unfortunately, most of these researches are limited by the poor spatial resolution of the characterizations.[12,13] This becomes particularly problematic as many 1D nanostructures have a large size distribution. Therefore, most of the previous research provides only averaged information about the 1D ZnO electronic structures. A couple of reports on the photoluminescence measurements of individual ZnO nanowires have become available recently.[14,15] However, these measurements do not provide simultaneous structural information and suffer from small signal-to-noise ratio.

In this study, we use an alternative approach—electron energy loss spectroscopy (EELS) performed inside a transmission electron microscope. The excellent spatial resolution (subnanometer) of this method allows us to study the electronic structure of individual ZnO nanowires, while simultaneously obtaining size and microstructure information. Two types of ZnO nanowire with different surface morphologies were synthesized. Size-dependent valence electron energy-loss spectra (VEELS) of individual wires are compared. Several surface-related features are observed in the loss spectra, and their physical origins are discussed. The results contribute to our general understanding of the electronic structure of the 1D ZnO nanostructures, one of the key factors in determining the feasibility of using these 1D nanostructures in various nano-optoelectronic devices.

The ZnO nanowires were synthesized by a thermal evaporation process using a vacuum tube furnace, as reported elsewhere.[16] Briefly, a ZnO and carbon-powder mixture with a ratio of 1:1 was used as the source material, which was loaded onto an alumina boat positioned at the center of the tube furnace. After evacuating the tube to $\sim 2 \times 10^{-3}$ Torr, the temperature of the chamber was ramped from 800 to 1100 °C with a heating rate of 20 °C/min at a constant flow of pure argon (100 sccm). In the second stage, a gas mixture of argon and oxygen with a ratio of 9:1 was introduced into the system immediately after the target temperature was reached, followed by a 3-h annealing. A total gas flow rate of 200 sccm (for sample a) and 100 sccm (for sample b) were maintained throughout the experiment. The as-synthesized nanowires were collected from the Au-coated Si substrates located downstream from the source.

The general morphology and microstructure of the nanowires were studied by scanning electron microscopy (SEM, LEO 1450VP) and transmission electron microscopy (TEM, Tecnai 20 ST, FEG 200 kV). The electron energy-loss measurements on the ZnO nanowires were performed using the Gatan GIF system attached to the TEM, operating at a primary energy of 200 keV, with an energy resolution of 0.7 eV. The spectra were acquired in TEM diffraction mode at small momentum transfer, with an angular resolution about 0.2 mrad. All of the spectra are calibrated using the zero loss peak position.

Two different types of ZnO nanowires were fabricated, as shown in the SEM images in Fig. 1. The nanowires in sample a have circular cross sections [see inset of Fig. 1(a)], whereas those in sample b have hexagonal cross sections [inset of Fig. 1(b)]. A size distribution of the nanowires is observed in both samples, the wire diameter ranging from

[a)]Electronic mail: liquan@phy.cuhk.edu.hk

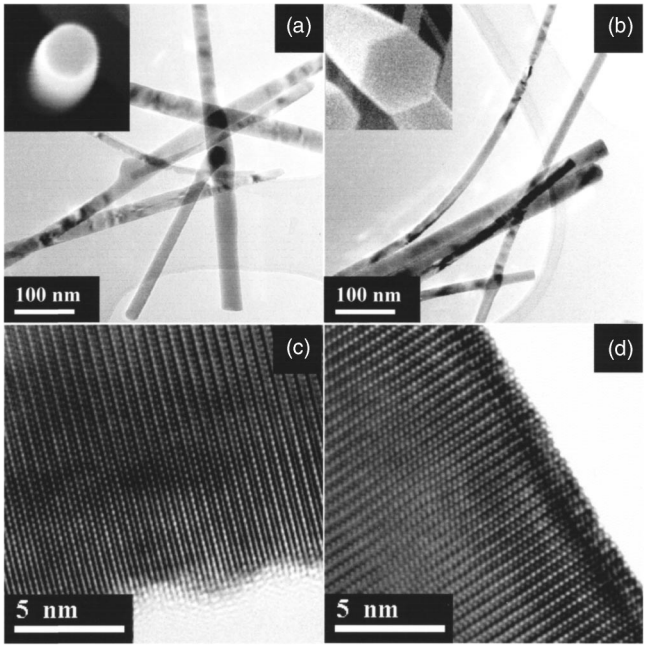

FIG. 1. (a) and (c) SEM images, low magnification TEM images, and corresponding high resolution TEM images of the ZnO nanowires in sample with circular cross section. (b) and (d) Sample with hexagonal cross section.

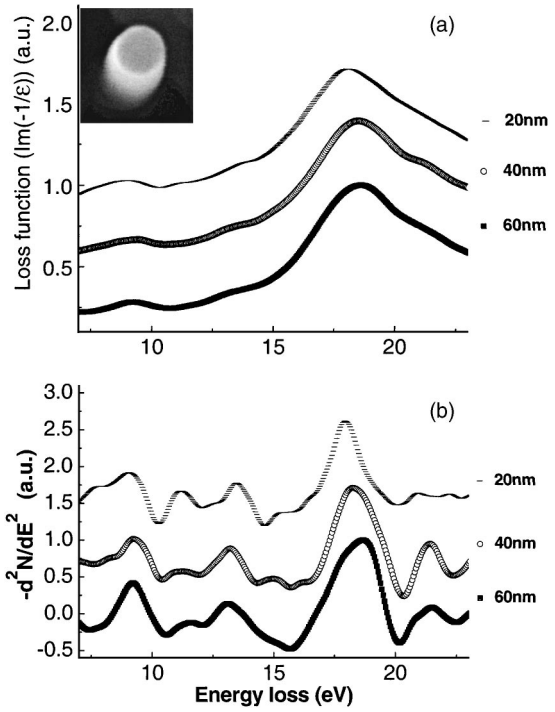

FIG. 2. (a) Loss functions $[\mathrm{Im}(-1/\varepsilon)]$ and (b) the corresponding second derivatives of the loss function for ZnO nanowires with different diameters and circular cross sections.

~20 to ~100 nm, as demonstrated in the low magnification TEM images in Figs. 1(a) and 1(b). The nanowires in both samples are single crystal with the hexagonal lattice, as suggested by transmission electron diffraction (not shown here) as well as by the high-resolution images [Figs. 1(c) and 1(d)]. The hexagonal [001] direction is identified as the growth direction for all of the nanowires. However, a rough surface is observed in sample a, in which the nanowires are of circular cross section [Fig. 1(c)], whereas the surface of the wires with hexagonal cross section appears to be much smoother and well defined [Fig. 1(d)].

Electron energy-loss spectroscopy was performed on several tens of ZnO nanowires of different sizes, from samples a and b, and the typical results are shown in Figs. 2 and 3, respectively. The loss function $[\mathrm{Im}(-1/\varepsilon)]$ of the nanowires with selected diameters (~20, ~40, and ~60 nm) in both samples are obtained by removing the plural scattering from the corresponding energy-loss spectra using a conventional Fourier-log deconvolution method.[17]

The loss functions of individual nanowires from sample a are shown in Fig. 2(a). The peak features in the low-loss spectra are magnified by performing a second-order differentiation of the loss function, as shown in Fig. 2(b). Several common features are observed in the nanowires with different sizes: a small peak at 9.5 eV, a shoulder at 13.5 eV, a dominant peak in the range from 18.1 to 18.8 eV and another shoulder at 21.8 eV. The intensity of a small peak at 11.5 eV is found to increase as the nanowire diameter decreases. The full width at half maximum of the dominant peak is also found to increase with the decreasing diameter. For the wire with the smallest diameter (~20 nm), the peak at 21.8 eV splits into two peaks centered at 20.8 and 22.1 eV, respectively. Simultaneously, the dominant peak is observed to shift to lower energy (from 18.8 to 18.1 eV).

The loss functions of individual nanowires from sample b are shown in Fig. 3(a). Features similar to those of sample a are observed, including the peak positions and the increase in oscillator strength of the 11.5 eV peak and broadening of the dominant peak as the nanowire diameter decreases. Nevertheless, neither a splitting of the 21.8 eV peak nor a shift of the dominant peak in the 20 nm nanowire is observed.

In the loss functions of all the ZnO nanowires in both samples, the dominant peak at about 18 eV is ascribed to a bulk plasmon excitation, which represents the collective os-

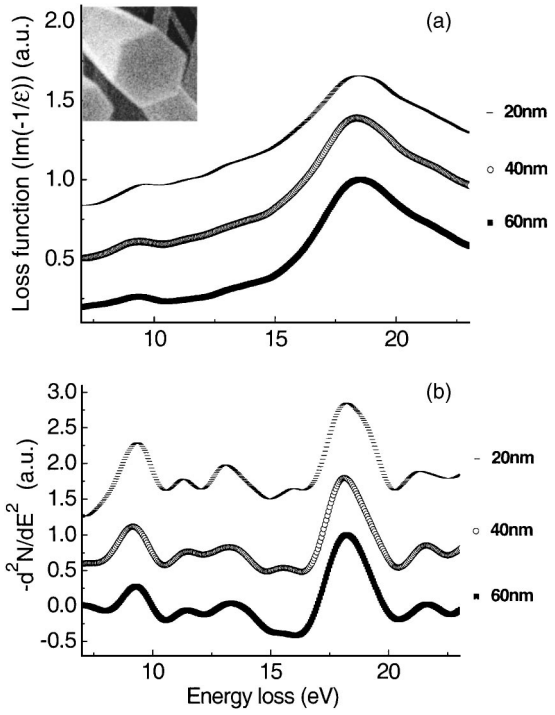

FIG. 3. (a) Loss functions $[\mathrm{Im}(-1/\varepsilon)]$ and (b) the corresponding second derivatives of the loss function for ZnO nanowires with different diameters and hexagonal cross sections.

cillation of the valence electrons excited by the incident fast electrons.[18] Several other common peaks at ~9.5, ~13.5, and ~21.8 eV are identified (respectively) as interband transitions from the O 2*p*, the Zn 3*d*, and the O 2*s* states in the valence band to unoccupied states in the conduction band. These peaks positions agree well with those of bulk ZnO,[19–21] indicating that the general electronic structures of the nanowires resemble their bulk counterpart.

On the other hand, subtle differences exist between the loss functions of the nanowires and of the bulk ZnO. The oscillator strength of the small peak at ~11.5 eV was observed to increase as the nanowire diameter decreases, revealing its size/surface-related origin. In fact, such 11.5eV peak has been reported as originating from the surface plasmon.[22] The increased oscillator strength of the ~11.5 eV peak also coincides with a decrease in that of the bulk plasmon, a consequence of the oscillator-strength sum rule. Its surface-plasmon interpretation is further confirmed by an EELS experiment performed at nonzero momentum transfer, which led to the disappearance of the 11.5 eV peak.[17,23]

Another size-related feature in the loss function of the nanowires is the gradual broadening of the bulk-plasmon peak as the nanowire diameter decreases. This effect can be explained by the increased scattering of the oscillating electrons by the wire surface when the surface to volume ratio increases,[24] a decrease in the relaxation time of the oscillating electrons leading to broadening of the bulk-plasmon peak.

It is interesting to note that the splitting of the 21.8 eV peak occurs only in nanowires with small diameter (less than 20 nm) and circular cross section. Such splitting had been predicted in work of Fumiyasu *et al.*, in which they found that the presence of O dangling bonds resulted in splitting of the O 2*s* state into two states, one with slightly higher energy than the original and the other slightly lower.[25] A large amount of these dangling bonds can be expected in the ZnO nanowires in sample a, in which the nanowires are of circular cross sections and thus no specific crystalline planes serve as the termination surfaces.

As a comparison, the ZnO nanowires in sample b have regular-hexagonal cross sections, and low index termination surfaces resulting in a significantly reduced number of dangling bonds at the nanowire surfaces. This is consistent with the EELS result of the nanowires in sample b: no splitting of the O 2*s* state is observed even for nanowire diameter down to 20 nm.

A redshift of the bulk-plasmon peak always occurs together with the splitting of the O 2*s* states (Figs. 2 and 3), suggesting a correlation between these two phenomena. As a matter of fact, single-electron interband transitions are known to couple with the plasmon oscillations, leading to a shift in the plasmon oscillation frequency.[26–28] When the interband transition occurs at an energy higher than the plasmon energy, i.e., $\omega_i > \omega_{p0}$, the plasmon energy is decreased below the original value due to this coupling effect. Such coupling effect is stronger if the interband transition energy is close to the plasmon oscillation energy.[29] As the O 2*s* transition occurs at an energy higher than the plasmon energy, and the splitting leads to the formation of new states in that energy range, the plasmon oscillation should lead to a redshift, consistent with the experimental observations.

In conclusion, two types of ZnO nanowires (circular versus hexagonal cross section) have been fabricated via thermal evaporation, by controlling the growth conditions. In general, the ZnO nanowires preserve the electronic structures of their bulk counterparts. Nevertheless, several size-related features are identified: a surface-plasmon oscillation at about 11.5 eV, whose oscillator strength increases as the nanowire diameter decreases, a broadening of the bulk-plasmon peak with decrease in wire diameter, and a splitting of the O 2*s* state together with the redshift of the bulk plasmon in small-diameter ZnO nanowires with circular cross sections. These effects can all be explained in terms of the increased surface/volume ratio when the diameter of the nanowire decreases. The experimental results strongly suggest that with careful control of the growth conditions (resulting in ZnO nanowires with hexagonal cross section and low-index surfaces), even nanowires with 20 nm diameter are of high electronic quality and can serve as effective building blocks for optoelectronic nanodevices.

The work described in this letter was fully supported by a grant from the RGC of HKSAR, China (Project No. 400904).

[1] M. Huang, S. Mao, H. Feick, H. Yan, Y. Y. Wu, H. Kind, E. Weber, R. Russo, and P. D. Yang, Science **292**, 1897 (2001).
[2] Z. L. Wang, X. Y. Kong, Y. Ding, P. Gao, W. L. Hughes, R. Yang, and Y. Zhang, Adv. Funct. Mater. **14**, 943 (2004).
[3] Y.-K. Tseng, C.-J. Huang, H.-M. Cheng, I.-N. Lin, K.-S. Liu, and I.-C. Chen, Adv. Funct. Mater. **13**, 811 (2003).
[4] Y. N. Xia, P. D. Yang, Y. G. Sun, Y. Y. Wu, B. Mayers, B. Gates, Y. D. Yin, F. Kim, and H. Q. Yan, Adv. Mater. (Weinheim, Ger.) **15**, 353 (2003).
[5] X. F. Duan, Y. Huang, R. Agarwal, and C. M. Lieber, Nature (London) **421**, 241 (2003).
[6] S. J. Chen, Y. C. Liu, J. G. Ma, D. X. Zhao, Z. Z. Zhi, Y. M. Lu, J. Y. Zhang, D. Z. Shen, and X. W. Fan, J. Cryst. Growth **240**, 467 (2002).
[7] Y. C. Kong, D. P. Yu, B. Zhang, W. Fang, and S. Q. Feng, Appl. Phys. Lett. **78**, 407 (2001).
[8] I. Shalish, H. Temkin, and V. Narayanamurti, Phys. Rev. B **69**, 245401 (2004).
[9] K. Ozawa, K. Sawada, Y. Shirotori, K. Edamoto, and M. Nakatake, Phys. Rev. B **68**, 125417 (2003).
[10] R. T. Girard, O. Tjernberg, G. Chiaia, S. Soderholm, U. O. Karlsson, C. Wigren, H. Nylen, and I. Lindau, Surf. Sci. **373**, 409 (1997).
[11] J. W. Chiou, K. P. Krishna Kumar, J. C. Jan, H. M. Tsai, C. W. Bao, W. F. Pong, F. Z. Chien, M.-H. Tsai, I.-H. Hong, R. Klauser, J. F. Lee, J. J. Wu, and S. C. Liu, Appl. Phys. Lett. **85**, 3220 (2004).
[12] Y. Y. Wang, S. C. Cheng, and V. P. Dravid, Micron **30**, 379 (1999).
[13] B. Rafferty and L. M. Brown, Phys. Rev. B **58**, 10326 (1998).
[14] J. A. Zapien, Y. Jiang, X. M. Meng, W. Chen, F. C. K. Au, Y. Lifshitz, and S. T. Lee, Appl. Phys. Lett. **84**, 1189 (2004).
[15] M. S. Gudiksen, L. J. Lauhon, J. Wang, D. C. Smith, and C. M. Lieber, Nature (London) **415**, 617 (2002).
[16] R. S. Wagner, *Whisker Technology*, edited by A. P. Levitt (Wiley-Interscience, New York, 1970).
[17] R. F. Egerton, *Electron Energy Loss Spectroscopy in the Electron Microscope* (Plenum, New York, 1986).
[18] P. David, Rev. Mod. Phys. **28**, 184 (1956).
[19] R. Dorn, H. Lüth, and M. Büchel, Phys. Rev. B **16**, 4675 (1977).
[20] R. L. Hengehold, R. J. Almassy, and F. L. Pedrotti, Phys. Rev. B **1**, 4784 (1970).
[21] R. A. Powell, W. E. Spicer, and J. C. Mcmenamin, Phys. Rev. B **6**, 3056 (1972).
[22] R. L. Hengehold and F. L. Pedrotti, Phys. Rev. B **6**, 3026 (1972).
[23] J. Fink, Adv. Electron. Electron Phys. **75**, 121 (1989).
[24] B. W. Reed, J. M. Chen, N. C. MacDonald, J. Silcox, and G. F. Bertsch, Phys. Rev. B **60**, 5641 (1999).
[25] O. Fumiyasu, S. R. Nishitani, and H. Adachi, Phys. Rev. B **63**, 045410 (2001).
[26] C. J. Powell, Phys. Rev. Lett. **15**, 852 (1965).
[27] C. B. Wilson, Proc. Phys. Soc. London **76**, 481 (1960).
[28] E. Zaremba and K. Sturm, Phys. Rev. Lett. **55**, 750 (1985).
[29] K. Strum, Adv. Phys. **31**, 1 (1982).